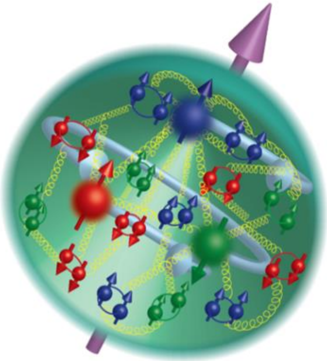

强子的形状因子抽取
及其相对论性密度诠释研究

陈毅

Based on:

[PRD 110, L091503 (2024)]
[JHEP 04, 132 (2025)]
[arXiv: 2512.06801 [hep-ph]]
[arXiv: 26xx.xxxx (to appear)]

thanks to:

Qing Chen, Feng-Kun Guo, Cédric Lorcé, Qun Wang, Bing-Song Zou

第五届强子与重味物理理论与实验联合研讨会(03.27-03.31, 2026)

Outline

1. Introduction and motivation
2. Neutrino-proton and antineutrino-proton elastic scattering
3. Relativistic axial-vector structure of a moving spin-1/2 hadron
4. Summary and outlook

致谢：

特别感谢“第五届强子与重味物理理论与实验联合研讨会”组委会！

谢谢您给了我一个交流和展示近期研究工作的机会！

Probing the internal structures of a hadron

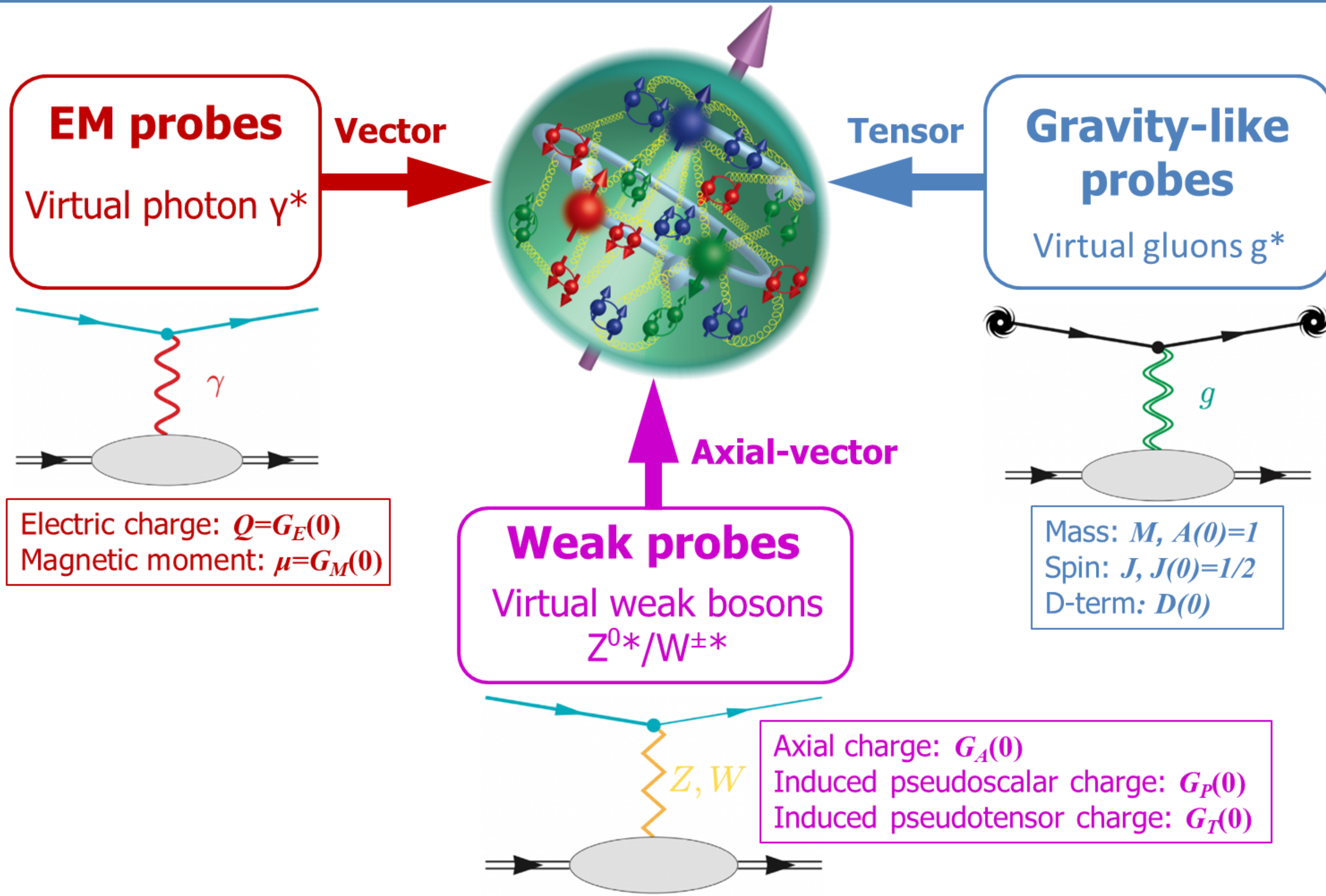

[M. Polyakov & P. Schweitzer, IJMPA 33(2018)1830025]
[Burkert, Elouadrhiri, Girod, Lorcé, Schweitzer, Shanahan. RMP 95, 041002 (2023)]...

Probing the internal structures of a hadron

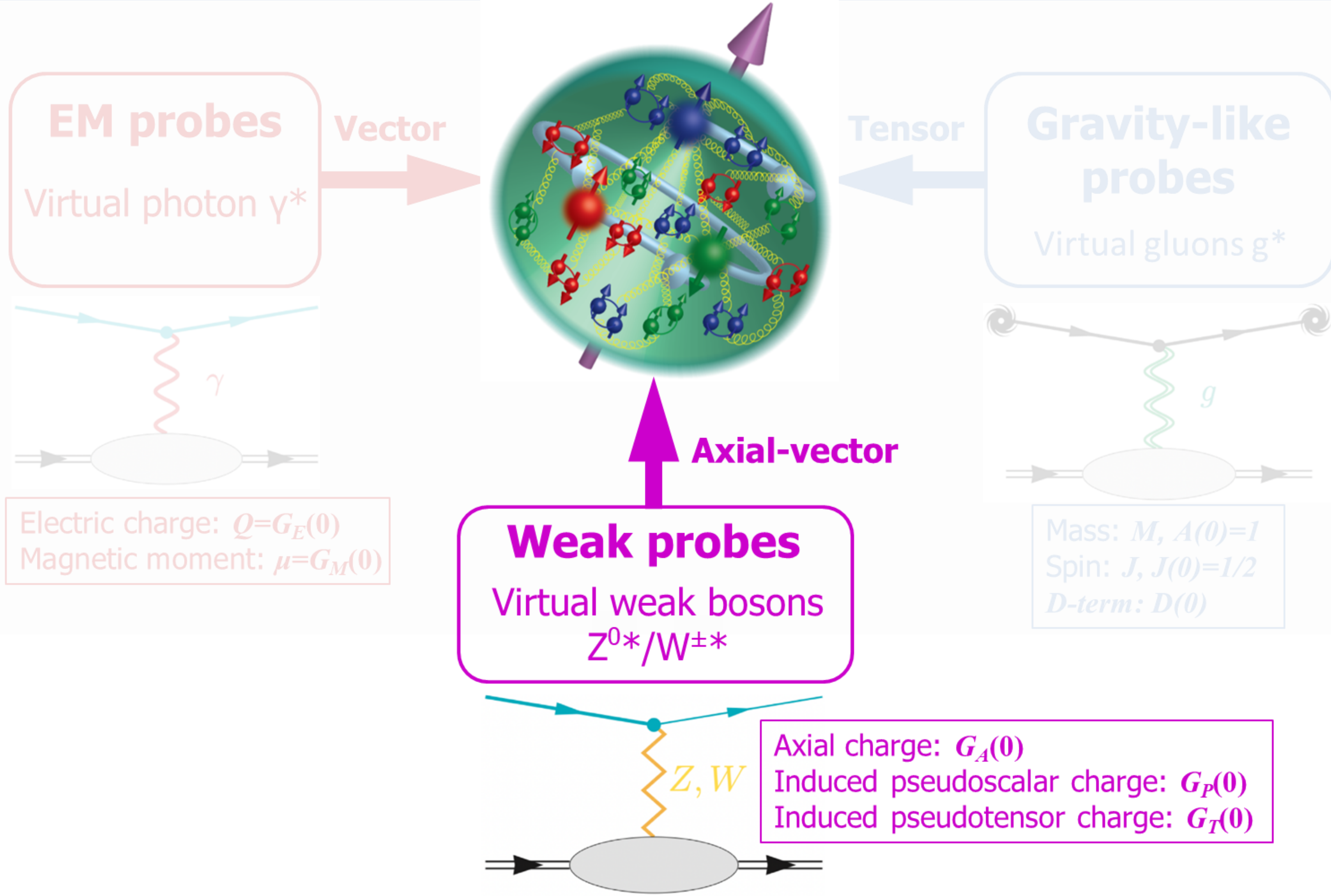

[M. Polyakov & P. Schweitzer, IJMPA 33(2018)1830025]
[V. Bernard, L. Elouadrhiri, & U. Meissner. J. Phys. G 28, R1 (2002)] ...

Structure dictates properties

- **Analogy:** **"Symmetry dictates interactions"** 对称性决定动力学

"Structure dictates properties" 结构决定性质

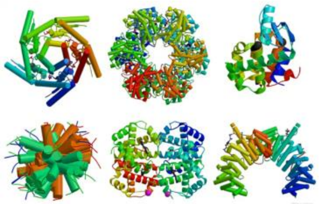

different proteins

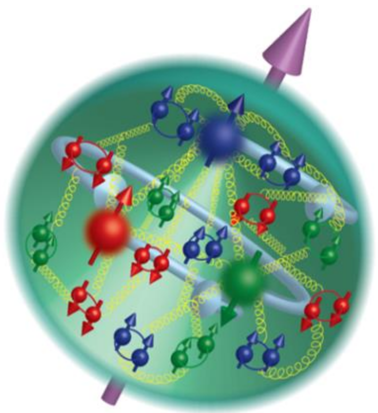

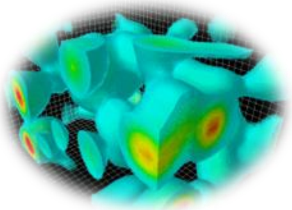

QCD vacuum

- **Hadron structures are highly non-trivial and complicated!**

(1). Hadron structures are closely associated with the nonperturbative QCD dynamics between the internal quark and gluon degrees of freedom.

(2). The QCD vacuum itself is also highly non-trivial, due to quantum fluctuations (loop effects, pair creations and annihilations), non-trivial topologies, instanton/sphaleron transitions, and etc.

(3). On top of the complicated QCD dynamics and non-trivial QCD vacuum structure, hadron structures are also affected by electromagnetic and weak interactions.

How to probe the internal structure of a system?

- **Classically, e.g. using x-ray diffraction on crystals:**

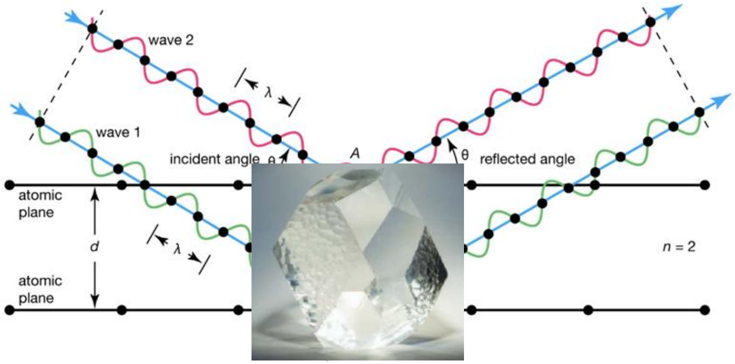

crystal

Diffraction pattern

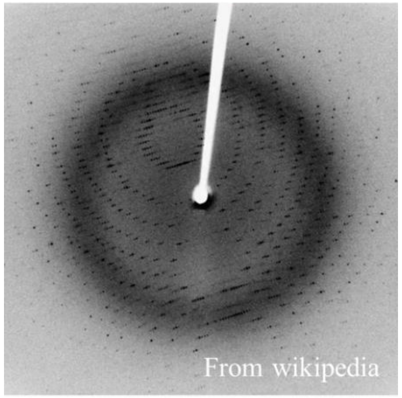

$\propto |\mathcal{A}_{\rm scatt}|^2$

Scattering amplitude: $\mathcal{A}_{\rm scatt} \propto F(\boldsymbol{q}) = \int \mathrm{d}^3 r \, e^{i\boldsymbol{q}\cdot\boldsymbol{r}} \rho(\boldsymbol{r}) \qquad \boldsymbol{q} = \boldsymbol{k} - \boldsymbol{k}'$

Form factor **Target distribution**

- **Experimentally, e.g. using modern Rutherford scattering:**

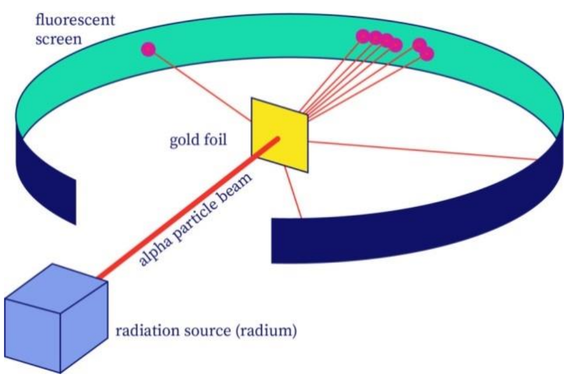

Rutherford alpha scattering experiment (1909)

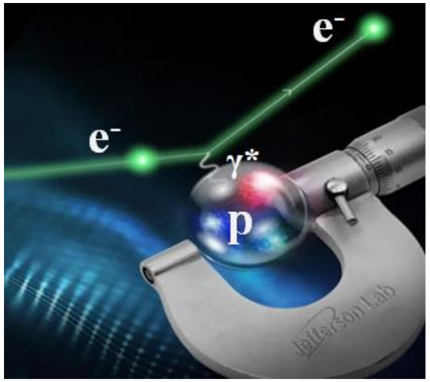

Jefferson lab e-p elastic scattering exps.

Elastic (anti)neutrino-proton scattering and why it?

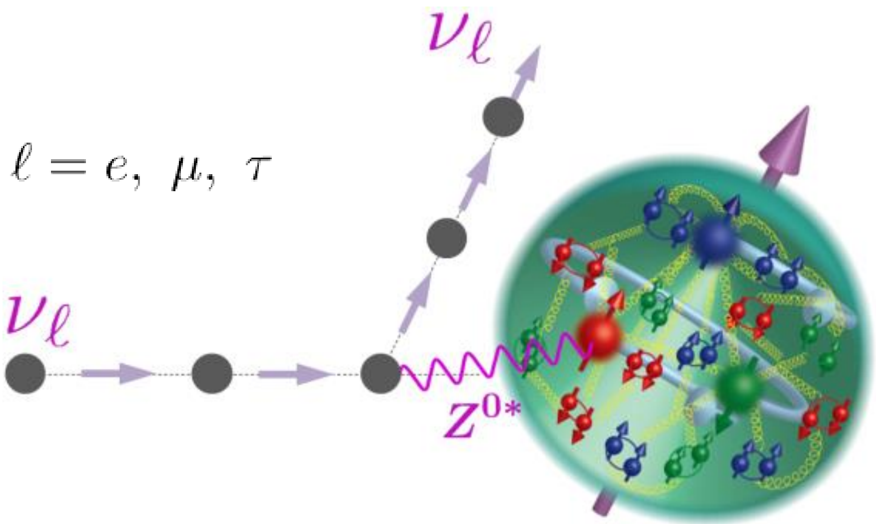

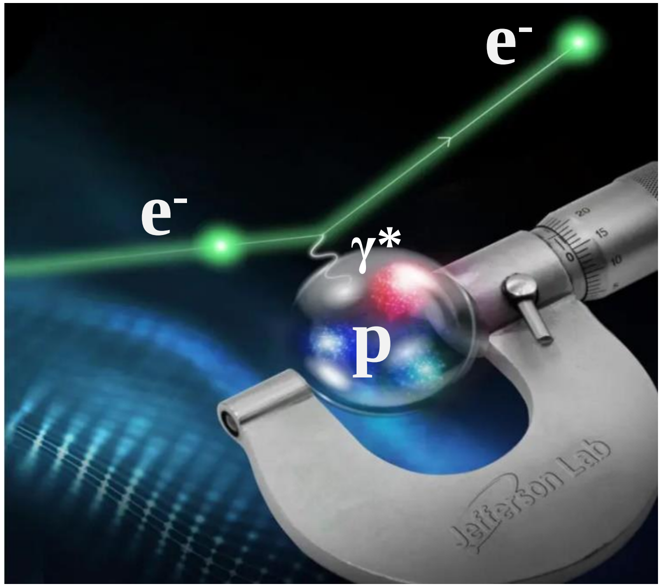

$\nu_\ell + N \to \nu_\ell + N$ $\ell^- + N \to \ell^- + N$

(1). By a simple analogy with the elastic electron-nucleon scattering.

(2). Very clean, since (anti)neutrinos participate only* in weak interactions.

(3). Key QCD bound-states (nucleons) in the weak sector: the weak content of the most important baryonic matter in Nature.

(4). Strangeness contributions to the nucleon spin → addressing the **spin crisis!**

(5). $G_A^s(0)$ **is only* accessible in weak neutral-current elastic scattering!**

(6). Constraining uncertainties in neutrino oscillation or P-violating exps.

The proton spin crisis

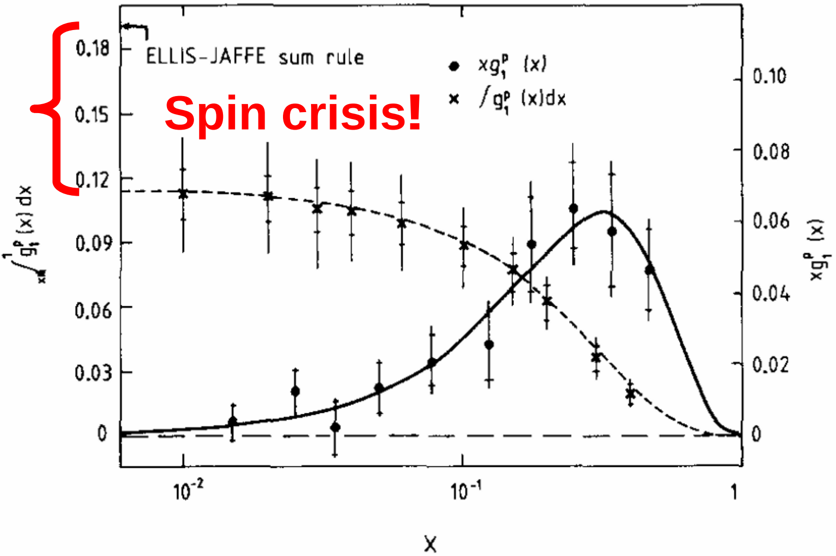

EMC experiment [PLB 206, 364 (1988)]

Total quark spin contribution:

$$\Delta\Sigma = \Delta u + \Delta d + \Delta s + \cdots$$
$$= G_A^u(0) + G_A^d(0) + G_A^s(0) + \cdots$$

$$G_A^Z(0) = \frac{1}{2}\left[\Delta u - \Delta d - \Delta s + \Delta c + \cdots\right]$$

→ **u and d quarks contribute only (14±9±21)% of the proton spin!**

$$\Delta\Sigma(\overline{Q^2} = 10.7\ \mathrm{GeV}^2) = 0.060 \pm 0.047 \pm 0.069$$
$$\int_0^1 \mathrm{d}x\, g_1^p(x) = 0.114 \pm 0.012 \pm 0.026$$

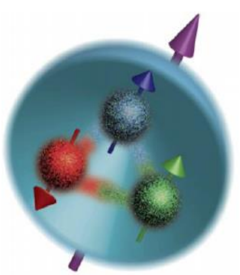

→

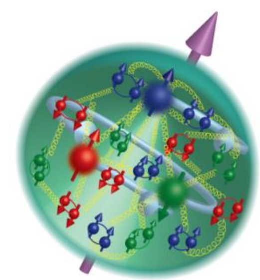

$$\frac{1}{2}\Delta\Sigma = \frac{1}{2}(\Delta u + \Delta d)$$

Ellis-Jaffe sum rule

$$\langle J_z\rangle^p = \frac{1}{2} = \frac{1}{2}\Delta\Sigma + \Delta G + L_z^q + L_z^g$$

Jaffe-Manohar IMF sum rule

Crucial for EICs/JLab experiments and scientific goals

- **One of the key scientific goals of EIC is to perform 3D tomography or imaging of the internal structures of nucleon/nuclei.**

Brookhaven National Laboratory

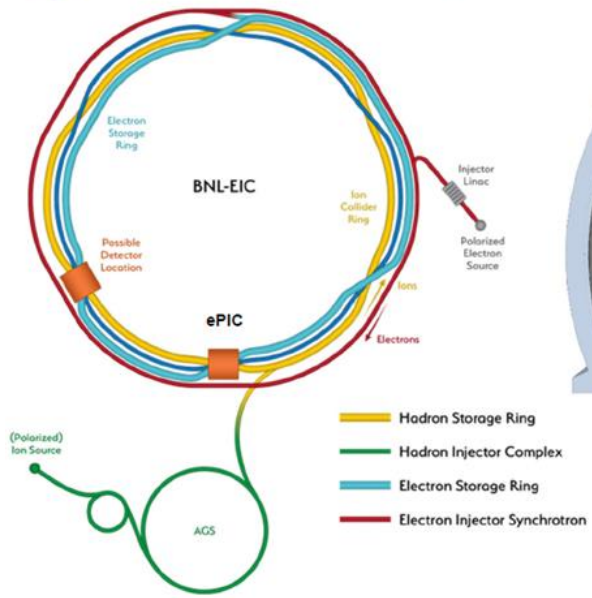

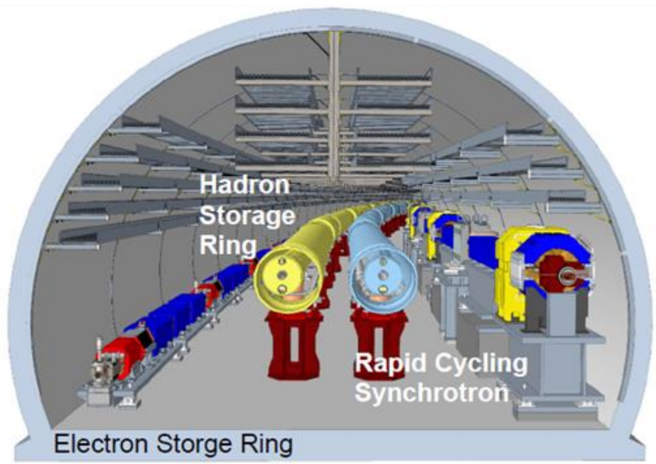

Jefferson Lab

EicC

- **Related to many big scientific questions:**

(1). Proton spin crisis and proton 3D spin structure;

(2). Proton charge radius puzzle;

(3). QCD confinement mechanism;

(4). Mass origin of the proton;

(5). Matter-antimatter asymmetry of the Universe (MAU/BAU); …

Some related facilities and experiments

Fermilab
(MiniBooNE, MINERvA, MicroBooNE, NOvA, ICARUS, ANNIE)

DUNE

JUNO

J-PARC
(Super-Kamiokande, T2K)

FASER
@ LHC near ATLAS

COHERENT SNS
@ ORNL(Oak Ridge)

…

Jefferson Lab

EicC

Brookhaven National Laboratory
EIC

…

Elastic (anti)neutrino-proton scattering

- **In general, a spin-1/2 hadron has 6 weak neutral form factors (FFs)**

$$\langle p', s' | \hat{j}^{\mu}_{Z}(0) | p, s \rangle = \bar{u}(p', s') \Gamma^{\mu}_{Z}(P, \Delta) u(p, s)$$

$$\Gamma^{\mu}_{Z}(P, \Delta) = \Gamma^{\mu}(P, \Delta) - \Gamma^{\mu}_{5}(P, \Delta),$$

$$\Gamma^{\mu}(P, \Delta) \equiv \gamma^{\mu} G^{Z}_{M} + \frac{P^{\mu}(G^{Z}_{E} - G^{Z}_{M})}{M(1+\tau)} + \frac{i\Delta^{\mu}}{2M} G^{Z}_{S},$$

$$\Gamma^{\mu}_{5}(P, \Delta) \equiv \left[\gamma^{\mu} G^{Z}_{A} + \frac{\Delta^{\mu}}{2M} G^{Z}_{P} - \frac{\sigma^{\mu\nu}\Delta_{\nu}}{2M} G^{Z}_{T} \right] \gamma^{5}.$$

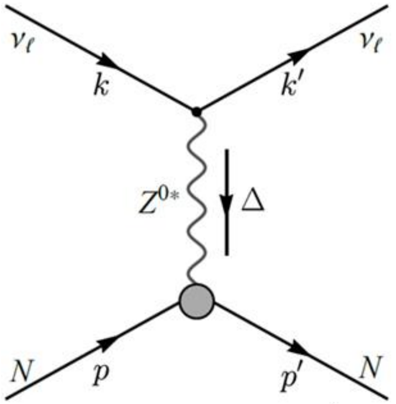

$$\nu_\ell N \to \nu_\ell N$$

$$\hat{j}^{\mu}_{Z}(x) \equiv \sum_{q} \hat{\bar{q}}(x) \gamma^{\mu} (g^{q}_{V} - g^{q}_{A}\gamma_5) \hat{q}(x)$$

$$q = u, d, s, c, b, t$$

$$u_i = u, c, t, \quad d_i = d, s, b$$

$$g^{u_i}_{A} = \frac{1}{2}, \quad g^{d_i}_{A} = -\frac{1}{2}$$

$$g^{u_i}_{V} = \frac{1}{2} - \frac{4}{3}\sin^2\theta_W, \quad g^{d_i}_{V} = -\frac{1}{2} + \frac{2}{3}\sin^2\theta_W$$

- **3 vector + 3 axial-vector weak neutral FFs**

$G^{Z}_{E,M,S}$ → **electric, magnetic, induced scalar**

$G^{Z}_{A,P,T}$ → **axial, induced pseudoscalar, induced pseudotensor**

[YC, Y. Li, C. Lorcé, & Q. Wang. PRD 110, L091503 (2024); JHEP 04, 132 (2025); 2512.06801 [hep-ph]]
[YC, Q. Chen, F.-K. Guo, Q. Wang, & B.-S. Zou. 26xx.xxxx (to appear)]

Differential cross sections at tree level

- **Elastic (anti)neutrino-proton scattering at tree level:**

$$\frac{d\sigma^{\pm}}{dQ^2} = \frac{G_F^2 M^2}{8\pi E_\nu^2}\left(\frac{M_Z^2}{M_Z^2+Q^2}\right)^2\left[A(Q^2) \pm \frac{s-u}{M^2}B(Q^2) + \frac{(s-u)^2}{M^4(1+\tau)}C(Q^2)\right]$$

$$A(Q^2) \equiv 4\tau\left[\left(\mathcal{F}_A^Z\right)^2 - \left(\mathcal{F}_T^Z\right)^2 + \tau\left(G_M^Z\right)^2 - \left(G_E^Z\right)^2\right],$$

$$B(Q^2) \equiv 4\tau G_A^Z G_M^Z,$$

$$C(Q^2) \equiv \frac{1}{4}\left[\left(\mathcal{F}_A^Z\right)^2 + \left(\mathcal{F}_T^Z\right)^2 + \tau\left(G_M^Z\right)^2 + \left(G_E^Z\right)^2\right].$$

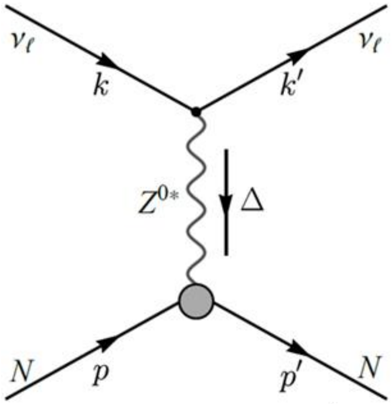

$\nu_\ell N \to \nu_\ell N$

- **Definition of some variables**

$$\Delta = p' - p = k - k'$$
$$P = (p' + p)/2$$
$$Q^2 = -\Delta^2 \geq 0$$
$$\tau \equiv Q^2/(4M^2)$$

$$\sigma^+ = \sigma(\nu p \to \nu p), \qquad \sigma^- = \sigma(\bar{\nu} p \to \bar{\nu} p)$$

$$\mathcal{F}_A^Z \equiv \sqrt{1+\tau}\, G_A^Z \qquad s \equiv (p+k)^2$$

$$\mathcal{F}_T^Z \equiv \sqrt{\tau(1+\tau)}\, G_T^Z \qquad u \equiv (k' - p)^2$$

- **Effectively, 4 FFs contribute explicitly to the differential cross sections.**

$$G_E^Z, \quad G_M^Z, \quad G_A^Z, \quad G_T^Z$$

- **In particular, nonzero $G_A^Z(Q^2)$ implies the P violation, and nonzero $G_T^Z(Q^2)$ implies both P and CP violations ⇨ matter-antimatter asymmetry/MAU.**

Weak-neutral axial-vector FFs of the nucleon: $G^Z_{A.P,T}(Q^2)$

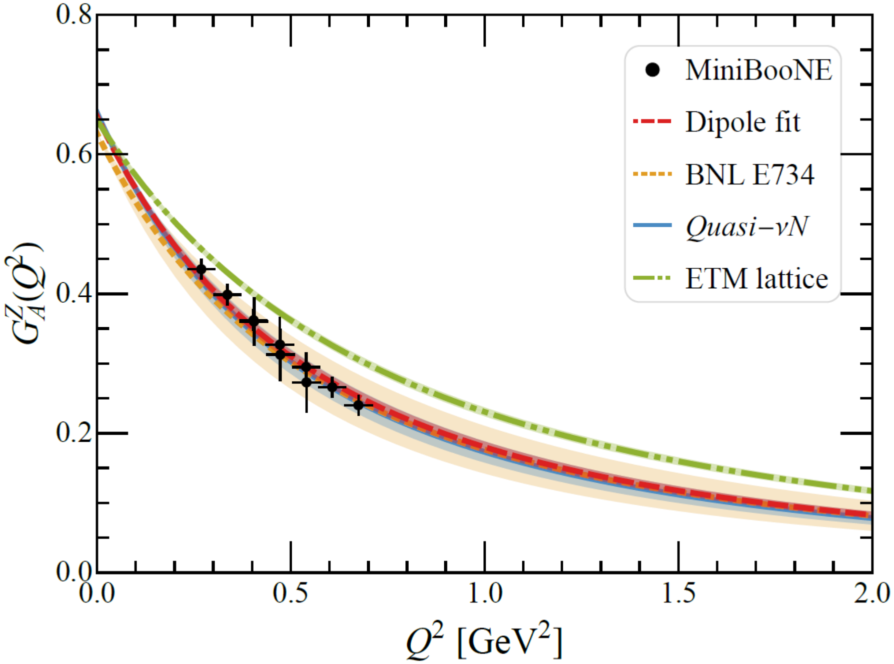

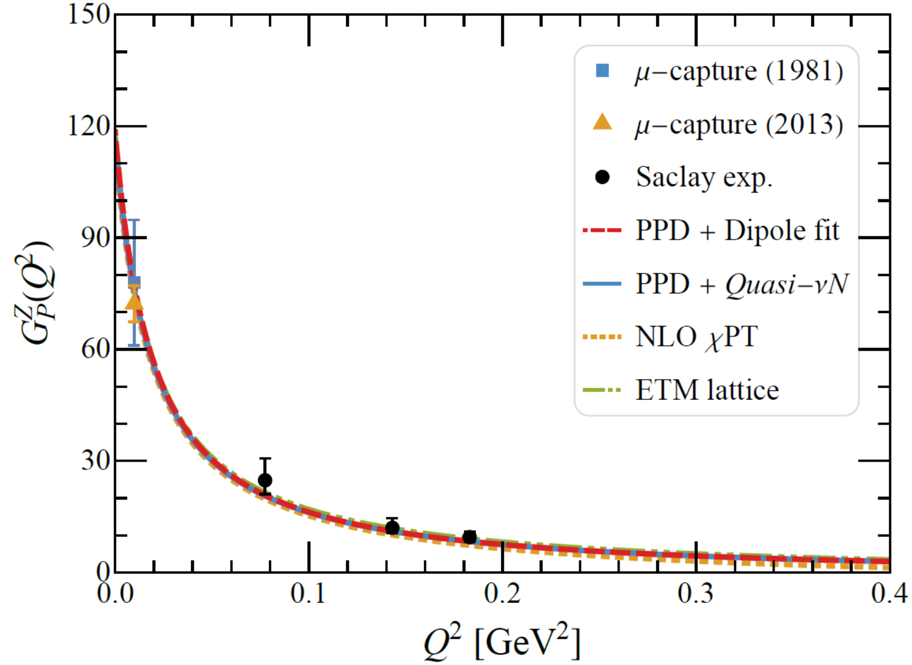

BNL E734
- [1]. Horstkotte, et al. Phys. Rev. D 25, 2743 (1982);
- [2]. Ahrens, et al. Phys. Rev. D 35, 785 (1987);

MiniBooNE
- [3]. Aguilar-Arevalo, et al. Phys. Rev. D 82, 092005 (2010);
- [4]. Aguilar-Arevalo, et al. Phys. Rev. D 91, 012004 (2015);

ETM lattice
- [5]. Alexandrou, et al. Phys. Rev. D 103, 034509 (2021);
- [6]. Alexandrou, et al. Phys. Rev. D 104, 074503 (2021);…

μ-capture
- [7]. Bardin, et al. Phys. Lett. B 104, 320 (1981);
- [8]. Andreev, et al. Phys. Rev. Lett. 110, 012504 (2013);

Saclay exp.
- [9]. Choi, et al. Phys. Rev. Lett. 71, 3927 (1993);

[Bernard, Kaiser & Meissner, PRD 50, 6899 (1994)]
[R. Sufian, K. Liu & D. Richards. JHEP 01, 136 (2020)]
[YC. JHEP 04, 132 (2025); 2512.06801 [hep-ph]]

Pion-pole dominance (PPD) hypothesis and scaling ansätz

- **PPD:** $$G_P^Z(Q^2) = \frac{4M^2}{M_\pi^2 + Q^2} G_A^Z(Q^2)$$ ← **PCAC and Goldberger-Treiman relations**

  pion pole

- **NLO ChPT (χPT):**

$$g_{\pi^\pm pn} = \frac{\sqrt{4\pi}(M_p + M_n)}{M_\pi} f_{\pi^\pm pn} \approx (13.22613 \pm 0.04369)$$

$$G_P^W(Q^2) = g_{\pi^\pm pn} \frac{2(M_p + M_n)F_\pi}{Q^2 + M_\pi^2} - 2G_A^W(0)\frac{(M_p + M_n)^2}{(M_A^W)^2} + \mathcal{O}(Q^2; M_\pi^2)$$

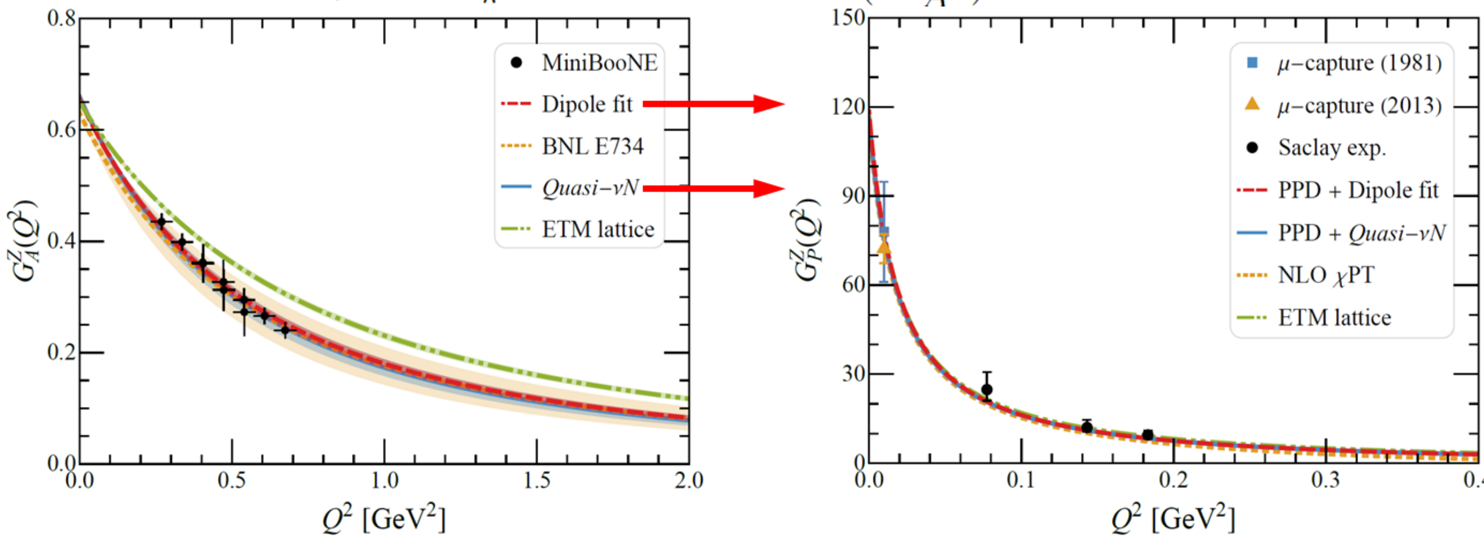

- **Induced pseudotensor FF (scaling ansätz):** $$G_T^Z(Q^2) = \kappa_T \cdot G_A^Z(Q^2), \quad \kappa_T \approx 0.1$$

[Y. Jang, R. Gupta, B. Yoon & T. Bhattacharya, PRL 124, 072002 (2020)]
[C. Alexandrou [ETM], et al. PRD 103, 034509 (2021)]
[Bernard, Kaiser & Meissner, PRD 50, 6899 (1994); Reinert et al. PRL 126, 092501 (2021)]
[M. Day & K. McFarland, PRD 86, 053003 (2012)]
[C. Chen, C. Fischer, C. Roberts & J. Segovia, PRD 105, 094022 (2022); EPJA 58, 206 (2022)]

Nucleon 3D mean-square axial radius $\langle r_A^2 \rangle \neq R_A^2$

- **Standard definition of 3D mean-square axial (charge) radius $\langle r_A^2 \rangle$:**

$$\langle r_A^2 \rangle \equiv \frac{\int \mathrm{d}^3 r \, r^2 \, J^0_{5,B}(\boldsymbol{r})}{\int \mathrm{d}^3 r \, J^0_{5,B}(\boldsymbol{r})}$$

$$\langle r_E^2 \rangle \equiv - \frac{6}{G_E(0)} \frac{\mathrm{d}G_E(Q^2)}{\mathrm{d}Q^2}\bigg|_{Q=0}$$

- **Naïve traditional definition of axial (charge) radius R_A^2, by a simple analogy with the traditional definition of the mean-square proton charge radius:**

$$R_A^2 \equiv - \frac{6}{G_A(0)} \frac{\mathrm{d}G_A(Q^2)}{\mathrm{d}Q^2}\bigg|_{Q^2=0}$$

Justification of the naïve 3D mean-square nucleon axial (charge) radius R_A^2 has never been rigorously discussed since 1986!

(for almost 40 years!!!)

[Meissner & Kaiser, PLB 180, 129 (1986)]
[Meissner & Kaiser & Weise, NPA 466, 129 (1986)]
[A1 Collaboration, PLB 468, 20 (1999)]
[Hill, et al. Rept. Prog. Phys. 81, 096301 (2018)]
[MINERvA Collaboration, Nature 614, 48 (2023)]
...

3D mean-square axial radius $\langle r_A^2 \rangle$ in the Breit frame

(1). Assuming G-parity invariance,

$$_N\langle p', s' | \hat{j}_5^\mu(0) | p, s\rangle_N = \bar{u}(p', s') \left[\gamma^\mu G_A + \frac{\Delta^\mu}{2M} G_P \right] \gamma^5 u(p, s)$$

Axial

Induced pseudoscalar

In the 3D BF: $_N\langle p', s' | \hat{j}_5^0(0) | p, s\rangle_N = 0 \quad \rightarrow \quad J_{5,B}^0(\boldsymbol{r}) = 0$

→ **Totally vanishing 3D axial charge distribution, thus no 3D axial radius!**

(2). Without assuming G-parity invariance,

$$_N\langle p', s' | \hat{j}_5^\mu(0) | p, s\rangle_N = \bar{u}(p', s') \left[\gamma^\mu G_A^Z + \frac{\Delta^\mu}{2M} G_P^Z - \frac{\sigma^{\mu\nu}\Delta_\nu}{2M} G_T^Z \right] \gamma^5 u(p, s)$$

Axial

Induced pseudoscalar

Induced pseudo-tensor

In the 3D BF: $_N\langle p', s' | \hat{j}_5^0(0) | p, s\rangle_N = \sqrt{1+\tau}\,(\boldsymbol{\sigma} \cdot i\boldsymbol{\Delta})\, G_T^Z(\boldsymbol{\Delta}^2)$

P-odd

→ **1). 3D axial charge distribution is related to $G_T^Z(Q^2)$ rather than $G_A^Z(Q^2)$;**
2). It is parity-odd, thus there is no 3D mean-square axial radius!

Nucleon 3D axial charge distribution & axial radius $\langle r_A^2 \rangle$

In either cases, i.e. $G_T^Z(Q^2) = 0$ or $G_T^Z(Q^2) \neq 0$, 3D mean-square axial radius for a spin-1/2 hadron does not exist. This is dictated by the parity symmetry.

$$J^0_{5,B}(\boldsymbol{r}) = \int \frac{\mathrm{d}^3\Delta}{(2\pi)^3} e^{-i\boldsymbol{\Delta}\cdot\boldsymbol{r}} \frac{(\boldsymbol{\sigma}\cdot i\boldsymbol{\Delta})}{2M} G_T^Z(\boldsymbol{\Delta}^2) \qquad \int \mathrm{d}^3 r\, J^0_{5,B}(\boldsymbol{r}) = 0$$

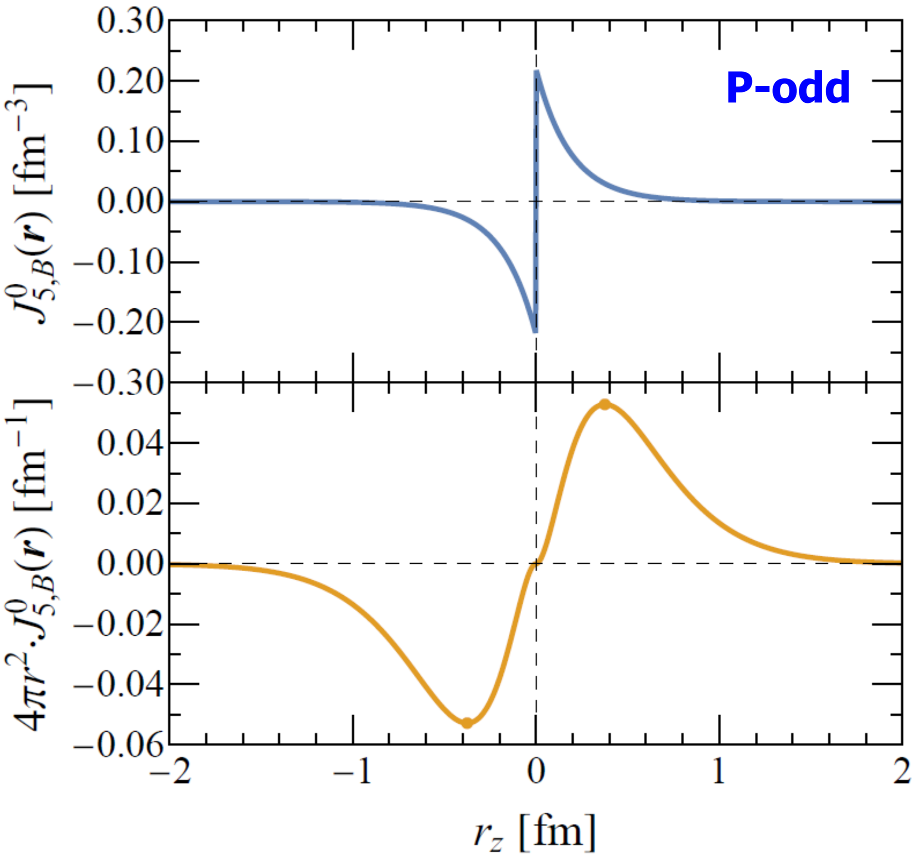

[YC, Y. Li, C. Lorcé, and Q. Wang. PRD 110, L091503 (2024)]
[YC. JHEP 04, 132 (2025); 2512.06801 [hep-ph]]

Different nature of axial-vector and vector four-currents

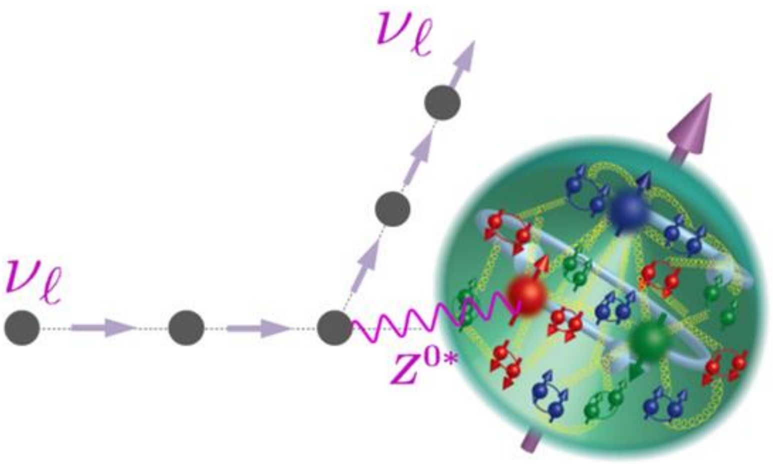

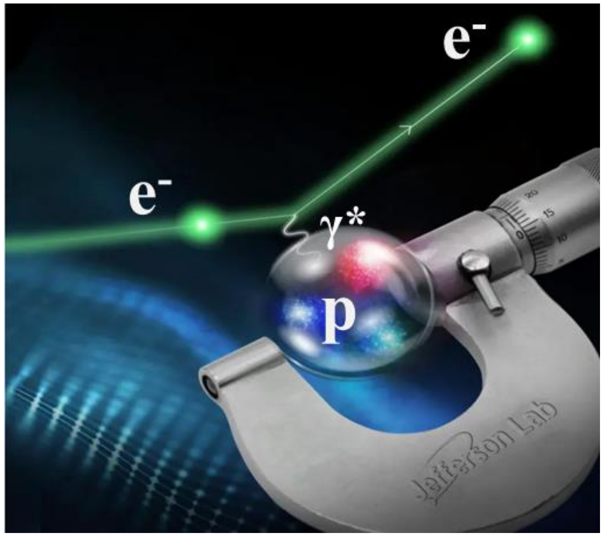

$P_\mu \Gamma_5^\mu = 0$ $\quad \hat{j}_5^\mu = \hat{\bar{\psi}}\gamma^\mu\gamma^5\hat{\psi}$

spacelike four-current J_5^μ

↓ **intrinsic part**

$\boldsymbol{J}_5 = 2\boldsymbol{S}$ **twice of spin distribution**

$\Delta_\mu \Gamma^\mu = 0$ $\quad \hat{j}^\mu = \hat{\bar{\psi}}\gamma^\mu\hat{\psi}$

timelike four-current J^μ

↓ **intrinsic part**

$J^0 = \rho_{\rm ch}$ **electric charge distribution**

$P = (p' + p)/2$

$\Delta = p' - p$

[C. Lorcé, PRL 125, 232002 (2020)]
[YC, & Cédric Lorcé, PRD 106, 116024 (2022)]
[YC, & Cédric Lorcé, PRD 107, 096003 (2023)] ...
[YC, Y. Li, C. Lorcé, & Q. Wang. PRD 110, L091503 (2024)]
[YC. JHEP 04, 132 (2025); 2512.06801 [hep-ph]]

Relation between spin tensor and axial-vector four-current

- **Using the QCD equations of motion, one can explicitly show that**

$$\hat{S}^{\mu\alpha\beta}(x) = \frac{1}{2}\epsilon^{\mu\alpha\beta\lambda}\hat{\bar{\psi}}(x)\gamma_\lambda\gamma^5\hat{\psi}(x) = \frac{1}{2}\epsilon^{\mu\alpha\beta\lambda}\hat{j}_{5\lambda}$$

with the axial-vector four-current operator given by $\hat{j}_5^\mu(x) \equiv \hat{\bar{\psi}}(x)\gamma^\mu\gamma^5\hat{\psi}(x)$

[E. Leader & C. Lorcé. Physics Reports 541, 163 (2014)]

- **Spin density operator and spin vector density (spin current)**

$$\hat{S}^i(x) = \frac{1}{2}\epsilon^{ijk}\hat{S}^{0jk} = \frac{1}{2}\hat{j}_5^i(x) \quad \rightarrow \quad \boldsymbol{S} = \frac{1}{2}\boldsymbol{J}_5$$

→ **Spin vector density S** is so closely related to the **axial current density J_5.**

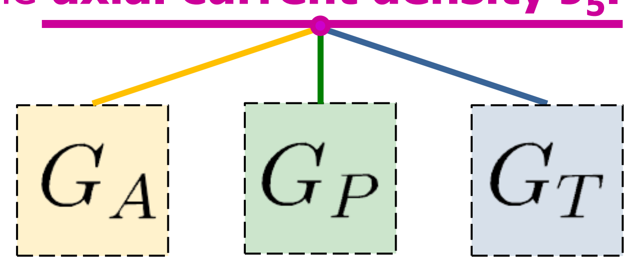

[Lorcé & Mantovani, & Pasquini. PLB 776, 38 (2018)]
[YC, Y. Li, C. Lorcé, & Q. Wang. PRD 110, L091503 (2024)]
[YC. JHEP 04, 132 (2025); 2512.06801 [hep-ph]]

Relativistic 3D intrinsic spin structure of the nucleon

◆ **3D BF spin vector density** $\boldsymbol{S}_B(\boldsymbol{r}) = \frac{1}{2}\boldsymbol{J}_{5,B}(\boldsymbol{r})$

$$\boldsymbol{J}_{5,B}(\boldsymbol{r}) = \int \frac{\mathrm{d}^3\Delta}{(2\pi)^3}\, e^{-i\boldsymbol{\Delta}\cdot\boldsymbol{r}} \left\{ \left[\boldsymbol{\sigma} - \frac{\boldsymbol{\Delta}(\boldsymbol{\Delta}\cdot\boldsymbol{\sigma})}{4P_B^0(P_B^0+M)}\right] G_A^Z(\boldsymbol{\Delta}^2) - \frac{\boldsymbol{\Delta}(\boldsymbol{\Delta}\cdot\boldsymbol{\sigma})}{4MP_B^0} G_P^Z(\boldsymbol{\Delta}^2) \right\}$$

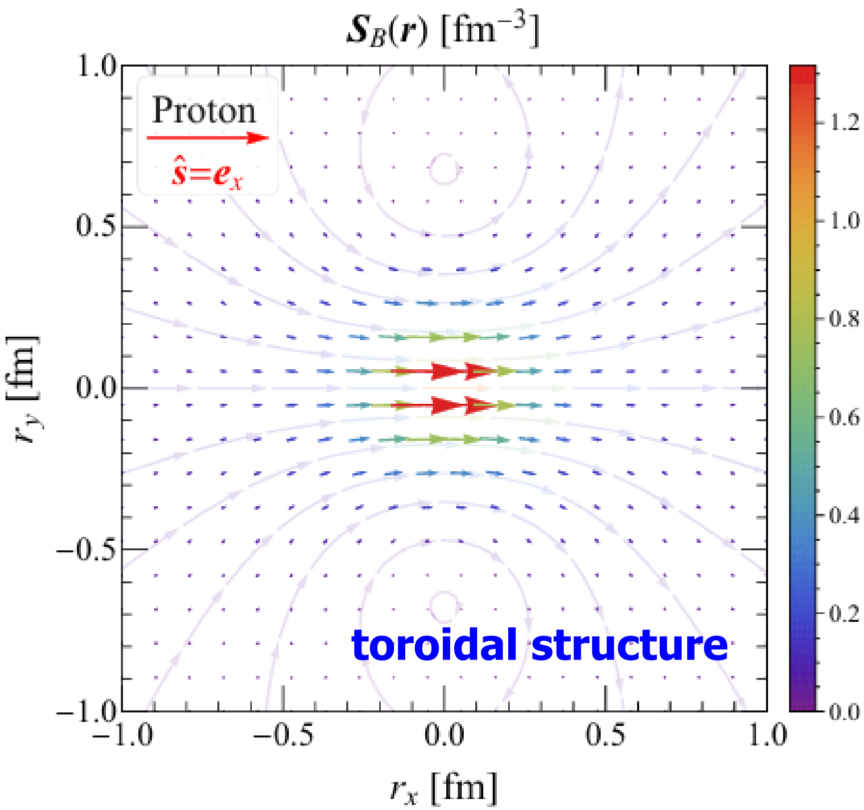

■ **Input from MiniBooNE @ Fermilab (anti)neutrino data:**

$G_A^Z(Q^2)$: MiniBooNE data;
$G_P^Z(Q^2)$: MiniBooNE data of G_A^Z (Q^2) + PPD (pion pole dominance);

■ **Multipole decomposition:**

$$\boldsymbol{S}_B(\boldsymbol{r}) = \boldsymbol{S}_B^{(M)}(\boldsymbol{r}) + \boldsymbol{S}_B^{(Q)}(\boldsymbol{r})$$

Up-down: mirror-symmetric

Left-right: mirror-antisymmetric

[MiniBooNE: PRD 82, 092005 (2010); PRD 91, 012004 (2015)]
[YC, Y. Li, C. Lorcé, Q. Wang. PRD 110, L091503 (2024); YC. JHEP 04, 132 (2025); 2512.06801]
[Sufian et al. JHEP 01, 136 (2020)]
[P. Neumann-Cosel et al. PRL 133, 233502 (2024)]

Toroidal structure of ^{208}Pb & proton

PHYSICAL REVIEW LETTERS **133,** 232502 (2024)

Editors' Suggestion | Featured in Physics

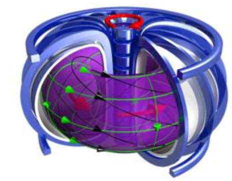

Candidate Toroidal Electric Dipole Mode in the Spherical Nucleus ^{58}Ni

P. von Neumann-Cosel,[1,*] V. O. Nesterenko,[2,3,†] I. Brandherm,[1] P. I. Vishnevskiy,[2,4] P.-G. Reinhard,[5] J. Kvasil,[6] H. Matsubara,[7,8] A. Repko,[9] A. Richter,[1] M. Scheck,[10,11] and A. Tamii[7]

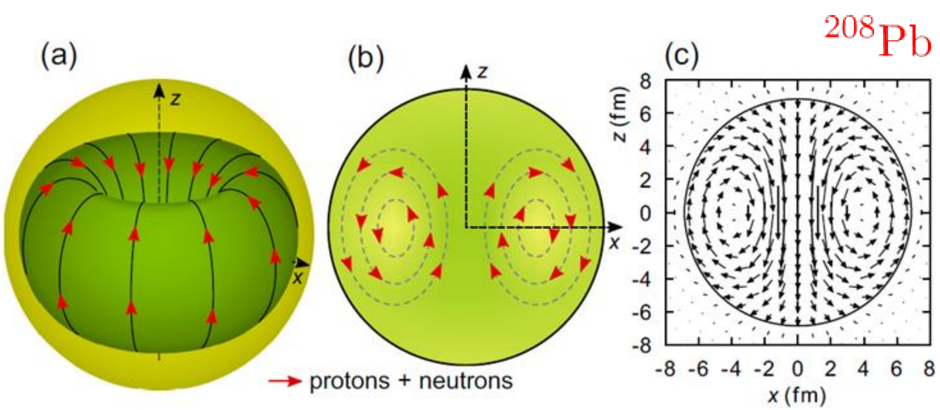

FIG. 1. Nuclear toroidal excitations. (a) Schematic view and (b) its cut in the *x*-*z* plane. (c) Same as (b) for the toroidal mode predicted in the nucleus ^{208}Pb [14]. The arrows mark the current along stream lines and their length is a measure of the current density.

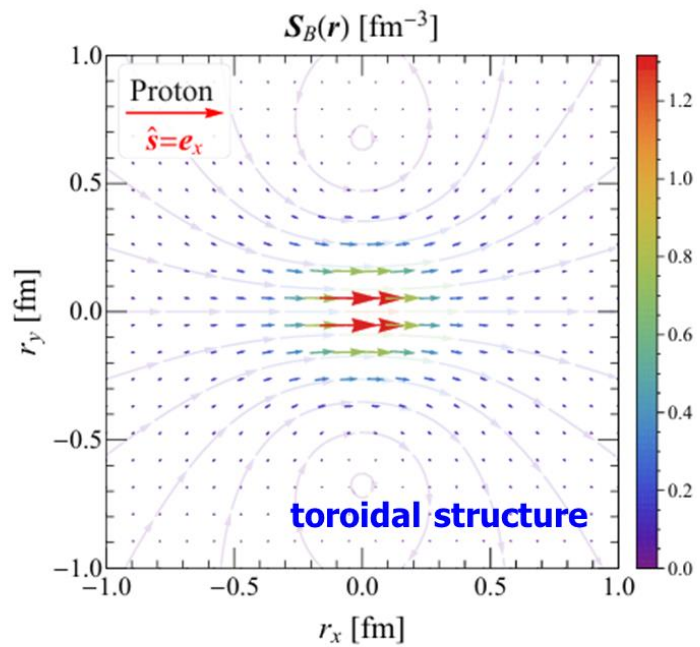

➡ Nucleon intrinsic spin structure is naturally of toroidal structure!

[P. Neumann-Cosel et al. PRL 133, 233502 (2024)]
[YC, Y. Li, C. Lorcé, Q. Wang. PRD 110, L091503 (2024); YC. JHEP 04, 132 (2025); 2512.06801]

Nucleon 3D mean-square spin radius $\langle r^2_{\rm spin}\rangle$

- Physically meaningful **3D mean-square spin radius**:

$$\langle r^2_{\rm spin}\rangle \equiv \frac{\int d^3r\, r^2\, \hat{\boldsymbol{s}}\cdot \boldsymbol{S}_B(\boldsymbol{r})}{\int d^3r\, \hat{\boldsymbol{s}}\cdot \boldsymbol{S}_B(\boldsymbol{r})} = R_A^2 + \frac{1}{4M^2}\left[1+\frac{2G_P^Z(0)}{G_A^Z(0)}\right]$$

Model-independent!

Based on **recent lattice QCD results** and **PPD hypothesis**, one can show that

$$\frac{G_P(0)}{G_A(0)} \gg 1$$

the last term $\frac{1}{2M^2}\frac{G_P(0)}{G_A(0)}$ **actually plays an dominant role!**

- Recently, R_A^2 was measured with high-precision by the **MINERvA Collaboration** at Fermilab. **[MINERvA Collaboration, Nature 614, 48 (2023)]**

- However, $\boldsymbol{R_A^2}$ **alone is not enough** to fix the meaningful 3D mean-square spin radius $\langle r^2_{\rm spin}\rangle$. **One still needs to determine the ratio $\boldsymbol{G_P^Z(0)/G_A^Z(0)}$.**

- This **provides an additional key motivation for ongoing lattice QCD and model calculations or future experimental measurements** of the nucleon induced pseudoscalar form factor $\boldsymbol{G_P^Z(Q^2)}$.

Covariant Lorentz transformations (based on Poincaré symmetry)

- **Axial-vector four-current case:**

$$\langle p', s'|\hat{j}_5^{\mu}(0)|p, s\rangle = \sum_{s'_B, s_B} \underbrace{D^{\dagger(j)}_{s's'_B}(p'_B, \Lambda) D^{(j)}_{s_B s}(p_B, \Lambda)}_{\text{Wigner rotation}} \underbrace{\Lambda^{\mu}{}_{\nu}}_{\text{Lorentz mixing}} \langle p'_B, s'_B|\hat{j}_5^{\nu}(0)|p_B, s_B\rangle$$

- **Exactly the same angular conditions as before* for the Wigner rotation angle θ:**

$$\cos\theta = \frac{P^0 + M(1+\tau)}{(P^0+M)\sqrt{1+\tau}}, \qquad \sin\theta = -\frac{\sqrt{\tau}P_z}{(P^0+M)\sqrt{1+\tau}}$$

- **Elastic frame (EF) axial-vector four-current distributions:**

$$J^0_{5,\text{EF}}(\boldsymbol{b}_\perp; P_z) = \int \frac{\mathrm{d}^2\Delta_\perp}{(2\pi)^2} e^{-i\boldsymbol{\Delta}_\perp\cdot\boldsymbol{b}_\perp} \left[\frac{(i\boldsymbol{\Delta}_\perp\cdot\boldsymbol{\sigma}_\perp)_{s's}}{2M} G^Z_T(\boldsymbol{\Delta}^2_\perp) + \left(\frac{P_z}{P^0}\right)(\sigma_z)_{s's} G^Z_A(\boldsymbol{\Delta}^2_\perp)\right]$$

$$J^z_{5,\text{EF}}(\boldsymbol{b}_\perp; P_z) = \int \frac{\mathrm{d}^2\Delta_\perp}{(2\pi)^2} e^{-i\boldsymbol{\Delta}_\perp\cdot\boldsymbol{b}_\perp} \left[\left(\frac{P_z}{P^0}\right)\frac{(i\boldsymbol{\Delta}_\perp\cdot\boldsymbol{\sigma}_\perp)_{s's}}{2M} G^Z_T(\boldsymbol{\Delta}^2_\perp) + (\sigma_z)_{s's} G^Z_A(\boldsymbol{\Delta}^2_\perp)\right]$$

} free from Winger spin rotation

$$\boldsymbol{J}^\perp_{5,\text{EF}}(\boldsymbol{b}_\perp; P_z) = \int \frac{\mathrm{d}^2\Delta_\perp}{(2\pi)^2} e^{-i\boldsymbol{\Delta}_\perp\cdot\boldsymbol{b}_\perp} \left\{-\frac{\boldsymbol{\Delta}_\perp(\boldsymbol{\Delta}_\perp\cdot\boldsymbol{\sigma}_\perp)_{s's}}{4P^0}\left[\frac{G^Z_A(\boldsymbol{\Delta}^2_\perp)}{P^0+M} + \frac{G^Z_P(\boldsymbol{\Delta}^2_\perp)}{M}\right] + \frac{\sqrt{P^2}}{P^0}\left[\cos\theta\,(\boldsymbol{\sigma}_\perp)_{s's} - \frac{(\boldsymbol{e}_z\times i\boldsymbol{\Delta}_\perp)_\perp}{2M\sqrt{\tau}}\sin\theta\,\delta_{s's}\right] G^Z_A(\boldsymbol{\Delta}^2_\perp)\right\}$$

} suffer from Winger spin rotation

[Durand, De Celles, Marr, PR 126, 1882 (1962)]
[Cédric Lorcé, PRL 125, 232002 (2020)]
[YC, and Cédric Lorcé, PRD 106, 116024 (2022); PRD 107, 096003 (2023)]*
[YC, Y. Li, C. Lorcé, & Q. Wang. PRD 110, L091503 (2024)]
[YC. JHEP 04, 132 (2025)]

Relativistic EF distributions of a moving proton

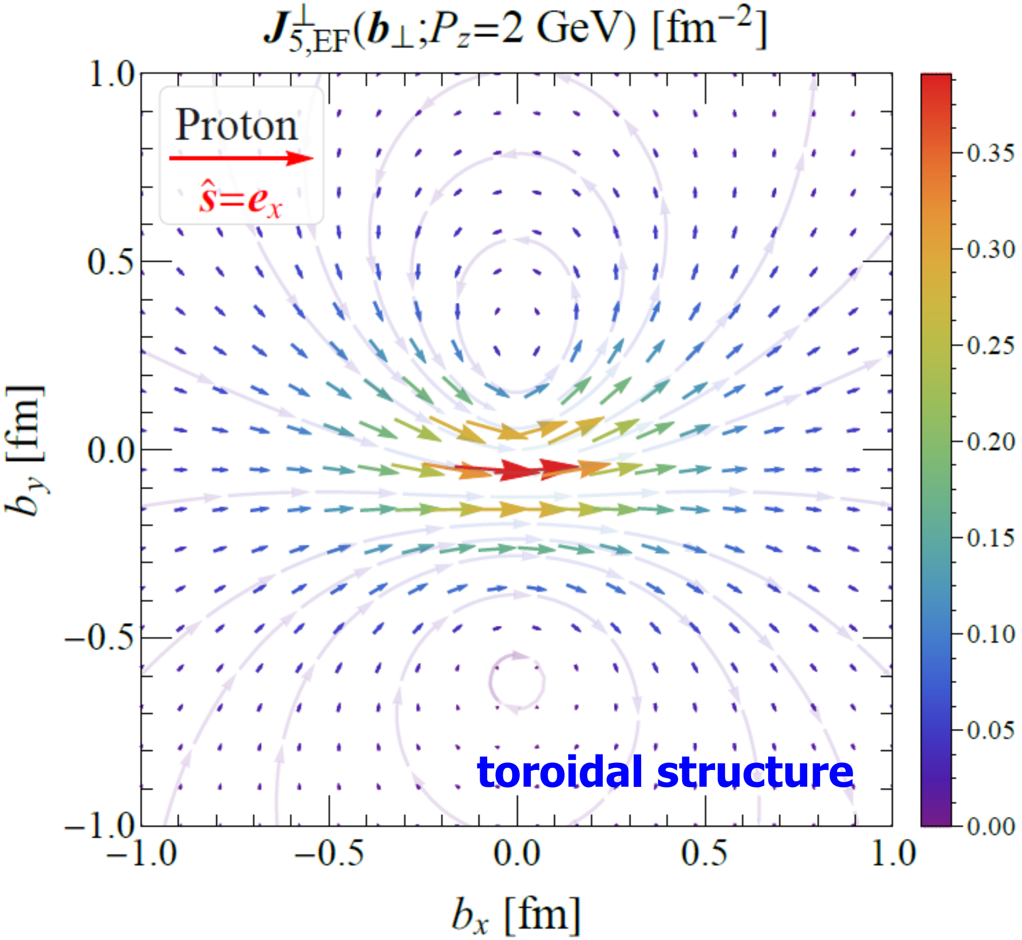

$$S^{\perp}_{\mathrm{EF}} = \frac{1}{2} J^{\perp}_{5,\mathrm{EF}}$$

$$J^{\perp}_{5,\mathrm{EF}} = J^{\perp(M)}_{5,\mathrm{EF}} + J^{\perp(D)}_{5,\mathrm{EF}} + J^{\perp(Q)}_{5,\mathrm{EF}}$$

← **Dipole contribution breaks explicitly the up-down symmetry!**

Up-down: mirror-asymmetric

Left-right: mirror-antisymmetric

- **Both $S_{\perp,\mathrm{EF}}$ and $J^{\perp}_{5,\mathrm{EF}}$ are free from Lorentz mixing effect but suffer from the spin Wigner rotation!**

[YC, Y. Li, C. Lorcé, and Q. Wang. PRD 110, L091503 (2024)]
[YC. JHEP 04, 132 (2025)]
[P. Neumann-Cosel et al. PRL 133, 233502 (2024)]

Proton's 2D transverse mean-square axial and spin radii

- **Axial radius** (for a longitudinally polarized, moving spin-1/2 hadron).

$$\langle b_A^2\rangle_{\mathrm{EF}}(P_z) = \frac{1}{2E_P^2} + \frac{2}{3}R_A^2$$

- **Longitudinal spin radius** (for a longitudinally polarized spin-1/2 hadron).

$$\langle b_{\mathrm{spin},L}^2\rangle_{\mathrm{EF}}(P_z) \equiv \frac{\int \mathrm{d}^2 b_\perp\, b^2\, S_{\mathrm{EF}}^z(\boldsymbol{b}_\perp; P_z)}{\int \mathrm{d}^2 b_\perp\, S_{\mathrm{EF}}^z(\boldsymbol{b}_\perp; P_z)} = \frac{2}{3}R_A^2$$

- **Transverse spin radius** (for a transversely polarized spin-1/2 hadron).

$$\langle b_{\mathrm{spin},T}^2\rangle_{\mathrm{EF}}(P_z) = \frac{2}{3}R_A^2 + \frac{1}{2M^2}\frac{G_P(0)}{G_A(0)} - \frac{1}{2M(E_P+M)} + \frac{1}{2E_P^2}$$

Conclusion: **the second-class current contribution [associated with $G_T^Z(Q^2)$], although explicitly included, does not contribute in fact to the mean-square axial and spin radii.**

[YC, Y. Li, C. Lorcé, & Q. Wang. PRD 110, L091503 (2024)]
[YC. JHEP 04, 132 (2025)]

Relativistic light-front (LF) distributions

- **In the IMF limit ($P_z \to \infty$):** $J^{+}_{5,\mathrm{LF}}(\boldsymbol{b}_\perp; P^+) = J^{0}_{5,\mathrm{EF}}(\boldsymbol{b}_\perp; \infty) = J^{z}_{5,\mathrm{EF}}(\boldsymbol{b}_\perp; \infty)$
- **Mean-square LF radii:**

$$\langle b_A^2 \rangle_{\mathrm{LF}}(P^+) = \langle b^2_{\mathrm{spin},L} \rangle_{\mathrm{LF}}(P^+) = \frac{2}{3} R_A^2$$

$$\langle b^2_{\mathrm{spin},T} \rangle_{\mathrm{LF}}(P^+) = \frac{2}{3} R_A^2 + \frac{1}{2M^2} \frac{G_P^Z(0)}{G_A^Z(0)}$$

~ independent of G_T^Z
(second-class current)

- **Scaled transverse LF axial current distribution:**

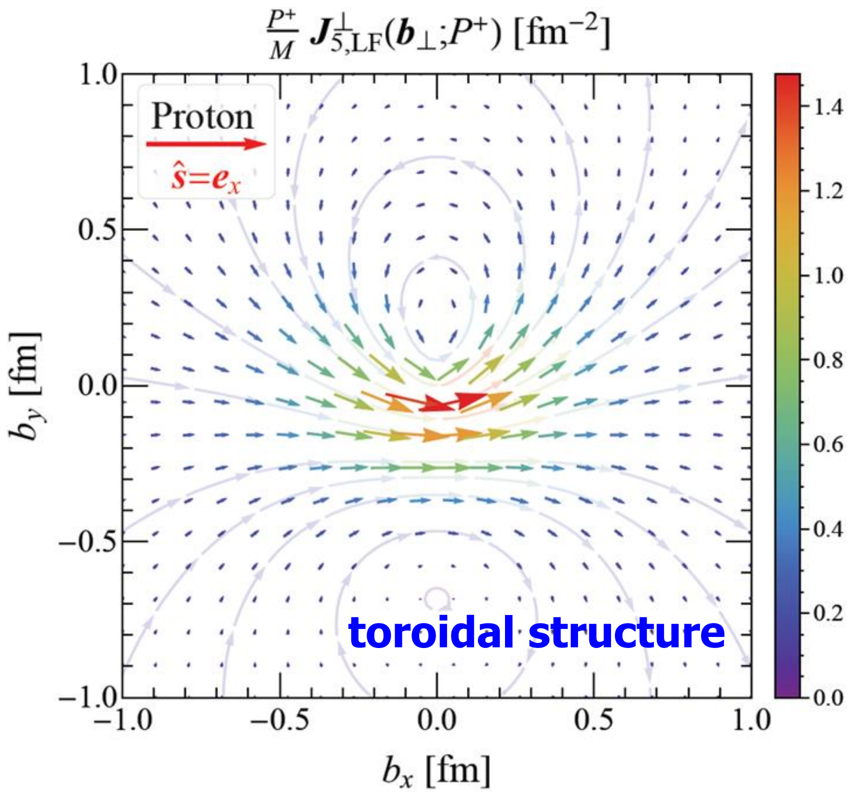

$$\boldsymbol{S}^{\perp}_{\mathrm{LF}} = \frac{1}{2} \boldsymbol{J}^{\perp}_{5,\mathrm{LF}}$$

Transversely polarized proton

Up-down: mirror-asymmetric

Left-right: mirror-antisymmetric

[YC, Y. Li, C. Lorcé, and Q. Wang. PRD 110, L091503 (2024); YC. JHEP 04, 132 (2025)]
[P. Neumann-Cosel et al. PRL 133, 233502 (2024)]

LF amplitudes via EF amplitudes at proper IMF limit

Conjecture. *Any light-front (LF) amplitudes for well-defined LF distributions in principle can be explicitly reproduced from the corresponding elastic frame (EF) amplitudes in the proper infinite-momentum frame (IMF) limit.*

This conjecture has been verified independently in:
(1). Electromagnetic four-current case;
(2). Polarization-magnetization and energy-momentum tensor cases;
(3). Axial-vector four-current case (with/without G_T^Z);
...

supporting LaMET?
(X. Ji, F. Yuan, Y. Zhao, Y. Liu, ...)

◆ EF amplitudes

$$\mathcal{A}^0_{\text{EF}} = 2P^0\left[\frac{(i\boldsymbol{\Delta}_\perp\cdot\boldsymbol{\sigma}_\perp)}{2M}G_T^Z(\boldsymbol{\Delta}_\perp^2)+\frac{P_z}{P^0}\sigma_z G_A^Z(\boldsymbol{\Delta}_\perp^2)\right],$$

$$\mathcal{A}^z_{\text{EF}} = 2P^0\left[\frac{P_z}{P^0}\frac{(i\boldsymbol{\Delta}_\perp\cdot\boldsymbol{\sigma}_\perp)}{2M}G_T^Z(\boldsymbol{\Delta}_\perp^2)+\sigma_z G_A^Z(\boldsymbol{\Delta}_\perp^2)\right],$$

$$\boldsymbol{\mathcal{A}}^\perp_{\text{EF}} = 2\sqrt{P^2}\left[\frac{P^0+M(1+\tau)}{(P^0+M)\sqrt{1+\tau}}\boldsymbol{\sigma}_\perp+\frac{(\boldsymbol{e}_z\times i\boldsymbol{\Delta}_\perp)_\perp}{2M}\frac{P_z}{(P^0+M)\sqrt{1+\tau}}\right]G_A^Z(\boldsymbol{\Delta}_\perp^2) - \frac{\boldsymbol{\Delta}_\perp(\boldsymbol{\Delta}_\perp\cdot\boldsymbol{\sigma}_\perp)}{2}\left[\frac{G_A^Z(\boldsymbol{\Delta}_\perp^2)}{P^0+M}+\frac{G_P^Z(\boldsymbol{\Delta}_\perp^2)}{M}\right],$$

◆ LF amplitudes

$$\mathcal{A}^+_{\text{LF}} = 2P^+\left[\frac{(i\boldsymbol{\Delta}_\perp\cdot\boldsymbol{\sigma}_\perp)_{\lambda'\lambda}}{2M}G_T^Z(\boldsymbol{\Delta}_\perp^2)+(\sigma_z)_{\lambda'\lambda}G_A^Z(\boldsymbol{\Delta}_\perp^2)\right],$$

$$\mathcal{A}^-_{\text{LF}} = 2P^-\left[\frac{(i\boldsymbol{\Delta}_\perp\cdot\boldsymbol{\sigma}_\perp)_{\lambda'\lambda}}{2M}G_T^Z(\boldsymbol{\Delta}_\perp^2)-(\sigma_z)_{\lambda'\lambda}G_A^Z(\boldsymbol{\Delta}_\perp^2)\right],$$

$$\boldsymbol{\mathcal{A}}^\perp_{\text{EF}} = 2M\left\{\left[(\boldsymbol{\sigma}_\perp)_{\lambda'\lambda}+\frac{(\boldsymbol{e}_z\times i\boldsymbol{\Delta}_\perp)_\perp}{2M}\delta_{\lambda'\lambda}\right]G_A^Z(\boldsymbol{\Delta}_\perp^2)-\frac{\boldsymbol{\Delta}_\perp(\boldsymbol{\Delta}_\perp\cdot\boldsymbol{\sigma}_\perp)_{\lambda'\lambda}}{4M^2}G_P^Z(\boldsymbol{\Delta}_\perp^2)\right\}$$

[Cédric Lorcé, PRL 125, 232002 (2020)]
[YC & Cédric Lorcé, PRD 106, 116024 (2022); PRD 107, 096003 (2023)]
[YC, Y. Li, C. Lorcé, Q. Wang. PRD 110, L091503 (2024)]
[YC. JHEP 04, 132 (2025)]

Summary and outlook

- **Hadron structures are highly non-trivial and complicated! They are closely related to many ongoing and new scientific programs and facilities. E.g. EIC, EicC, JLab 22 GeV upgrade, HAIF, etc.**

- **Neutrino/antineutrino elastic or quasi-elastic scatterings offer us a clean way to probe the internal structures of hadrons/nuclei in the weak sector. In particular, relativistic axial-vector and spin structures of nucleon are discussed in detail in terms of axial-vector FFs $G^Z_{A,P,T}(Q^2)$. New facilities, e.g. Fermilab, DUNE, JUNO, FASER, COHERENT, etc., can be well expected.**

- **Due to parity symmetry, physically meaningful 3D axial (charge) radius $\langle r_A^2 \rangle$ does not exist for any spin-1/2 hadrons. However, 3D mean-square nucleon spin radius $\langle r^2_{\text{spin}} \rangle$ is a physically meaningful quantity that better characterizes the size of spatial extension of weak content of nucleon.**

- **Any relativistic spatial distortions of a moving spinning hadron can be understood as a combination of Lorentz transformation and Wigner spin rotation. This is precisely protected by Poincaré symmetry.**

Thank you!

Backup: Covariant Lorentz transformation -- two key effects

- **Four-vector case** (e.g., electromagnetic four-current):

$$\langle p', s'|\hat{j}^\mu(0)|p, s\rangle = \sum_{s'_B, s_B} \underbrace{D^{\dagger(j)}_{s's'_B}(p'_B, \Lambda) D^{(j)}_{s_B s}(p_B, \Lambda)}_{\text{Wigner rotation}} \underbrace{\Lambda^\mu{}_\nu \langle p'_B, s'_B|\hat{j}^\nu(0)|p_B, s_B\rangle}_{\text{Lorentz mixing}}$$

- **Axial four-vector case** (e.g., axial-vector four-current):

$$\langle p', s'|\hat{j}^\mu_5(0)|p, s\rangle = \sum_{s'_B, s_B} \underbrace{D^{\dagger(j)}_{s's'_B}(p'_B, \Lambda) D^{(j)}_{s_B s}(p_B, \Lambda)}_{\text{Wigner rotation}} \underbrace{\Lambda^\mu{}_\nu \langle p'_B, s'_B|\hat{j}^\nu_5(0)|p_B, s_B\rangle}_{\text{Lorentz mixing}}$$

- **Tensor case** (e.g., polarization-magnetization tensor):

$$\langle p', s'|\hat{P}^{\mu\nu}(0)|p, s\rangle = \sum_{s'_B, s_B} \underbrace{D^{\dagger(j)}_{s's'_B}(p'_B, \Lambda) D^{(j)}_{s_B s}(p_B, \Lambda)}_{\text{Wigner rotation}} \underbrace{\Lambda^\mu{}_\alpha \Lambda^\nu{}_\beta \langle p'_B, s'_B|\hat{P}^{\alpha\beta}(0)|p_B, s_B\rangle}_{\text{Lorentz mixing}}$$

(1). Lorentz mixing effect

boost $\Lambda^\mu{}_\nu$

$$\begin{pmatrix} \tilde{J}^0_{\text{EF}} \\ \tilde{J}^z_{\text{EF}} \end{pmatrix} = \begin{pmatrix} \gamma & \beta\gamma \\ \beta\gamma & \gamma \end{pmatrix} \begin{pmatrix} \tilde{J}^0_B \\ \tilde{J}^z_B \end{pmatrix}$$ ~ momentum-space amplitudes

(2). Wigner rotation effect

Fundamental reason: boost generators of Lorentz group do not commutate!

$$\left[\hat{K}^i,\ \hat{K}^j\right] = -i\epsilon^{ijk}\hat{J}^k \longrightarrow$$ **Wigner rotation** $D^{(j)}_{s_B s}(p_B, \Lambda)$

[Durand, De Celles, Marr, PR 126, 1882 (1962)]
[Cédric Lorcé, PRL 125, 232002 (2020)]
[YC & Cédric Lorcé, PRD 106, 116024 (2022)]
[YC & Cédric Lorcé, PRD 107, 096003 (2023)]
[YC, Y. Li, C. Lorcé, & Q. Wang. PRD 110, L091503 (2024); JHEP 04, 132 (2025)]